Supporting Information

Defect-rich Fe doped NiS/MoS_2 heterostructured ultrathin nanosheets for efficient overall water splitting

Peng Liu[a], Jiawen Li[a], Jianyue Yan[a], and Wenbo Song[a,*]
[a] *College of Chemistry, Jilin University, Changchun 130012, P.R. China*

[*]Corresponding author.
E-mail address: wbsong@jlu.edu.cn

Contents:

1. Materials

Sodium molybdate dihydrate ($Na_2MoO_4 \cdot 2H_2O$, 99.0%), nickle nitrate hexahydrate [$Ni(NO_3)2 \cdot 6H_2O$, 99.0%], Ferric nitrate nonahydrate [$Fe(NO_3)_3 \cdot 9H_2O$, 99.0%], Nafion solution (5 wt%), N,N-dimethylformamide (DMF), Potassium hydroxide (KOH, 99.0%) and ethanol were purchased from Sinopharm Chemical Reagent Co. Ltd. 4,4-Bipyridine ($C_{10}H_8N_2$, 98%) and Pluronic® F-127 were purchased from Aladdin Industrial Corporation (Shanghai, China). All the reagents used in the experiment were of analytical grade and used without further purification.

2. Characterization

X-ray diffraction (XRD, PANalytical B.V. Empyrean Cu Ka radiation) was used to identify the crystal structure of prepared samples. Scanning electron microscopy (SEM, HITACHI SU8000) and transmission electron microscopy (TEM, JEOL JEM-2200FS) were utilized to investigate the morphology of samples. X-ray photoelectron spectroscopy (XPS) data were collected using ESCALAB 250 spectrometer with a monochromatic X-ray source with Al Kα excitation (1486.6 eV) under ultrahigh vacuum.

3. Electrode preparation and electrochemical measurement

Electrochemical measurements were performed with an electrochemical workstation (CHI 760E, CH Instruments Inc.) in 1 mol L^{-1} KOH aqueous solution. Saturated Calomel Electrode (SCE) and graphite rod were used as the reference and counter electrode, respectively. Typically, 4 mg of the catalyst powder was dispersed in 1mL of 50 vol % water and 50 vol % N,N-Dimethylformamide (DMF) mixed solvent, and the mixture was sonicated for 30 min. Then, 10 μL of the above solution was drop-cast onto the surface of a glassy carbon (GC) electrode. All the potential values were converted with respect to a reversible hydrogen electrode (RHE). Polarization curves were acquired under a potential sweep rate of 5 mV s^{-1}. Stability tests were performed in a potential range of -0.5 ~ 0 V for HER and 1.2 ~ 1.7 V for OER with a potential sweep rate of 150 mV s^{-1} for 1000 cycles. Current-time responses were operated by chronoamperometric measurements for 60000 s. The electrochemical

impedance spectroscopy (EIS) was carried out in the range from 100 KHz to 0.1 Hz with an AC amplitude of 5 mV. All the current density presented here was normalized to the geometrical area (0.0707 cm^2) of glassy carbon electrode with 95% iR correction.

4. synthetic method for control samples: Fe-doped NiS and Fe-doped MoS_2

9 mmol $Ni(NO_3)_2 \cdot 6H_2O$, 5 mmol 4,4-bipyridine and 1 mmol $Fe(NO_3)_3 \cdot 9H_2O$ were grinded to form evenly powder denoted as precursor A. 9 mmol Na_2MoO_4, 5 mmol 4,4-bipyridine and 1 mmol $Fe(NO_3)_3 \cdot 9H_2O$ were grinded to form evenly powder denoted as precursor B. Each of the above precursors was transferred into a corundum boat located at the center of a tubular furnace. Another corundum boat containing S powder was then placed in the upstream of precursor. Under a ramp rate of 3 °C min^{-1}, the tubular furnace was heated to 500 °C in N_2 atmosphere, and this temperature was maintained for 1h. The resultant products are denoted as Fe-doped NiS and Fe-doped MoS_2, respectively.

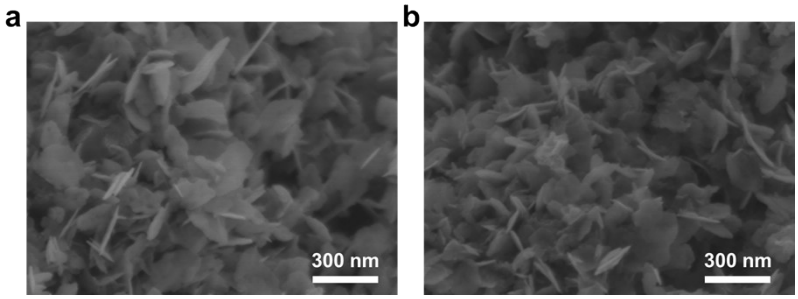

Fig. S1 SEM images of (a) 0.05Fe-Ni/Mo MOF and (b) 0.2Fe-Ni/Mo MOF

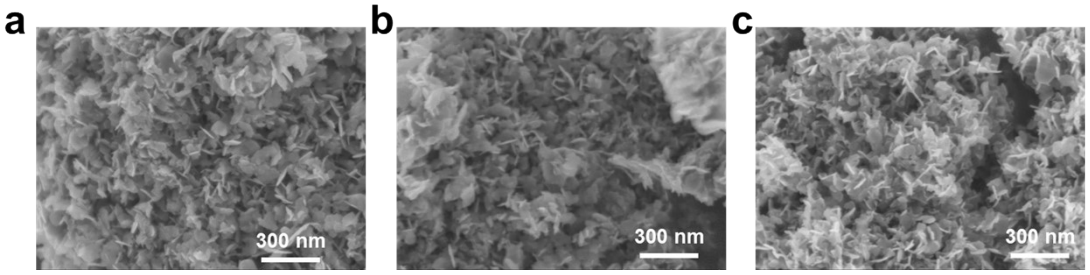

Fig. S2 SEM images of (a) NiS/MoS_2, (b) 0.05Fe-NiS/MoS_2 and (c) 0.2Fe-NiS/MoS_2

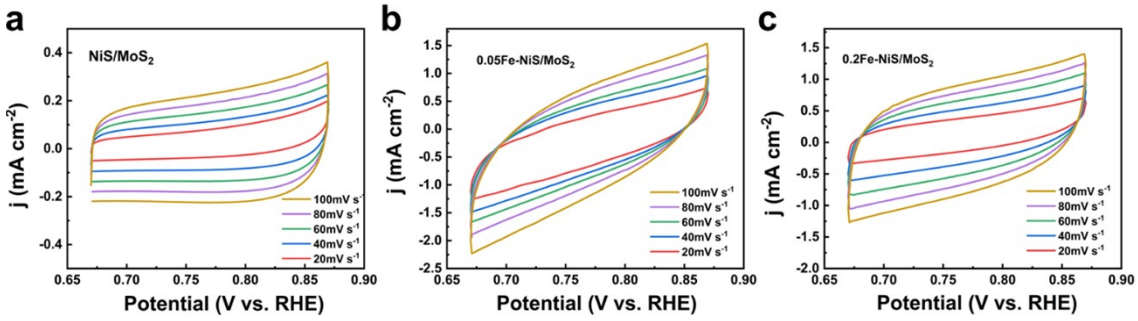

Fig. S3 CV curves of (a) NiS/MoS_2, (b) $0.05Fe\text{-}NiS/MoS_2$ and (c) $0.2Fe\text{-}NiS/MoS_2$ under different scan rates.

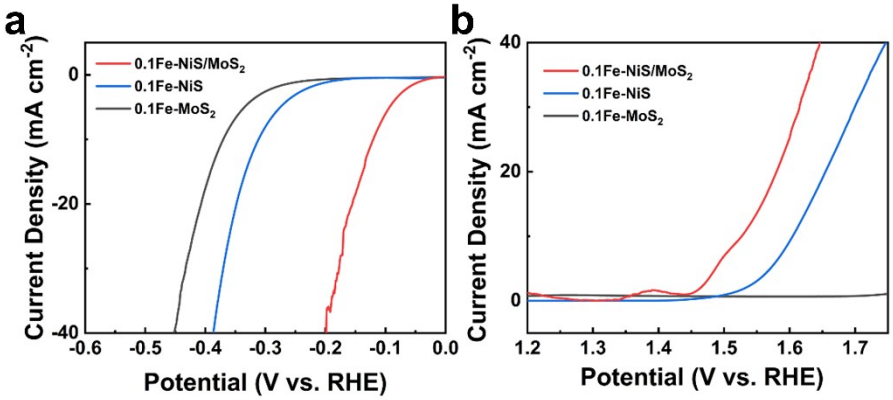

Fig. S4 HER (a) / OER (b) performance comparison of $0.1Fe\text{-}NiS/MoS_2$ with Fe-doped NiS and Fe-doped MoS_2

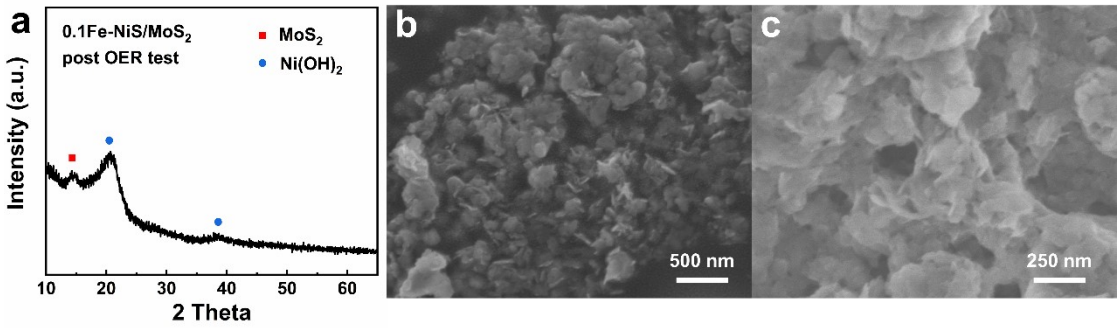

Fig. S5 XRD pattern (a) and SEM images (b, c) of $0.1Fe\text{-}NiS/MoS_2$ post 1000 cycles OER test.

Table S1. The ICP-AES result for samples with different Fe amount

elements	0.05Fe-NiS/MoS_2	0.1Fe-NiS/MoS_2	0.2Fe-NiS/MoS_2
Fe atom%	2.01	5.09	10.38
Ni atom%	41.26	45.89	39.73
Mo atom%	56.73	49.02	49.89

Table S2. HER/OER activity comparison with the recently reported Ni/Mo based sulfides.

Samples/substrates	HER η_{10} (mV)	HER Tafel slope (mV dec^{-1})	OER η_{10} (mV)	OER Tafel slope (mV dec^{-1})	reference
NiS/MoS_2/C (GC)	117	58	-	-	[1]
MoS_2/rGO/NiS (GC)	169	91.6	-	-	[2]
MoS_2|NiS|MoO_3	91	54.5	-	-	[3]
NiS/MoS_2 (CC)	174	70.2	-	-	[4]
MoS_2/NiS (GC)	244	97	350	108	[5]
Fe/C-doped-MoS_2/Ni_3S_2 (GC)	188	95	270	66	[6]
NiS_2/MoS_2 (GC)	135	82	293	102.3	[7]
NiS_2/MoS_2 (CC)	91	57.2	362 (η_{50})	117.3	[8]
0.1Fe-NiS/MoS_2 (GC)	120	69.0	297	54.7	This work

References

1 K. Tao, Y. Gong and J. Lin, *Electrochim. Acta*, 2018, **274**, 74-83.

2 G. Liu, K. Thummavichai, X. Lv, W. Chen, T. Lin, S. Tan, M. Zeng, Y. Chen, N. Wang and Y. Zhu, *Nanomaterials*, 2021, **11**.

3 C. Wang, B. Tian, M. Wu and J. Wang, *ACS Appl. Mater. Interfaces*, 2017, **9**, 7084-7090.

4 A. Long, W. Li, M. Zhou, W. Gao, B. Liu, J. Wei, X. Zhang, H. Liu, Y. Liu and X. Zeng, *Journal of Materials Chemistry A*, 2019, **7**, 21514-21522.

5 Q. Qin, L. Chen, T. Wei and X. Liu, 2019, **15**, 1803639.

6 X. Lv, G. Liu, S. Liu, W. Chen, D. Cao, T. Song, N. Wang and Y. Zhu, 2021, **11**, 340.

7 Q. Zhang, B. Liu, Y. Ji, L. Chen, L. Zhang, L. Li and C. Wang, *Nanoscale*, 2020, **12**, 2578-2586.

8 X. Wang, L. Li, Z. Wang, L. Tan, Z. Wu, Z. Liu, S. Gai and P. Yang, *Electrochimica Acta*, 2019, **326**, 134983.